Adaptation through proportion

2016 Phys. Biol. 13 046007

(http://iopscience.iop.org/1478-3975/13/4/046007)

Physical Biology

RECEIVED
19 April 2016

REVISED
12 June 2016

ACCEPTED FOR PUBLICATION
29 July 2016

PUBLISHED
16 August 2016

PAPER

Adaptation through proportion

Liyang Xiong[1,2,4], **Wenjia Shi**[2,4] **and Chao Tang**[1,2,3]

[1] School of Physics, Peking University, Beijing 100871, People's Republic of China
[2] Center for Quantitative Biology, Peking University, Beijing 100871, People's Republic of China
[3] Peking-Tsinghua Center for Life Sciences, Peking University, Beijing 100871, People's Republic of China
[4] These authors contributed equally to this work.

E-mail: tangc@pku.edu.cn

Keywords: adaptation, proportion, design principle, network

Supplementary material for this article is available online

Abstract

Adaptation is a ubiquitous feature in biological sensory and signaling networks. It has been suggested that adaptive systems may follow certain simple design principles across diverse organisms, cells and pathways. One class of networks that can achieve adaptation utilizes an incoherent feedforward control, in which two parallel signaling branches exert opposite but proportional effects on the output at steady state. In this paper, we generalize this adaptation mechanism by establishing a steady-state proportionality relationship among a subset of nodes in a network. Adaptation can be achieved by using any two nodes in the sub-network to respectively regulate the output node positively and negatively. We focus on enzyme networks and first identify basic regulation motifs consisting of two and three nodes that can be used to build small networks with proportional relationships. Larger proportional networks can then be constructed modularly similar to LEGOs. Our method provides a general framework to construct and analyze a class of proportional and/or adaptation networks with arbitrary size, flexibility and versatile functional features.

Introduction

Biological systems monitor external and internal signals and carry out appropriate responses using complex circuits. Behind the rich behaviors of natural and synthetic biological systems, such as bistable switch [1, 2], oscillation [3, 4], and spatial patterning [5, 6], are particular network motifs. Mapping out the relationship between function and architecture of biological networks and identifying the underlying design principles are of broad interest [7–12]. Among the biological functions, adaptation has been extensively studied in the context of various sensory and signaling systems [13–22]. Adaptation is the ability to transiently respond to a change of input stimuli, and then restore itself to the original steady state (figure 1(a)). This function allows the system to maintain a homeostasis and/or to respond to further changes of the input. Despite the fact that adaptive systems differ in different pathways and organisms, they share certain intrinsic similarities [23–25]. Previous studies have shown that only a limited number of network architectures can perform adaptation [24, 25]. Ma *et al* [25], by enumerating all possible three-node enzymatic regulatory networks, found that all adaptive three-node networks converge on two classes: a negative feedback loop with a buffer node (NFBLB) and an incoherent feedforward loop with a proportioner node (IFFLP). In the NFBLB class, an intermediate node integrates the error of the output node and thus buffers the change of output to help it adapt using integral feedback control. In the IFFLP class, the intermediate node responds to the input proportionally and offsets the influence of the input on the output. Both classes need only certain general constraints on few key parameters to carry out perfect adaptation. This work supports the idea that there exist general design principles behind biological systems. However, due to the complexity of computation, only the three-node networks were analyzed. Real biological systems are more complex; it is desirable and important to understand the structure and behavior of larger networks. One challenge facing us is to scale up computational methods to tackle large size networks. In this study, we develop a rigorous framework to hierarchically construct proportional

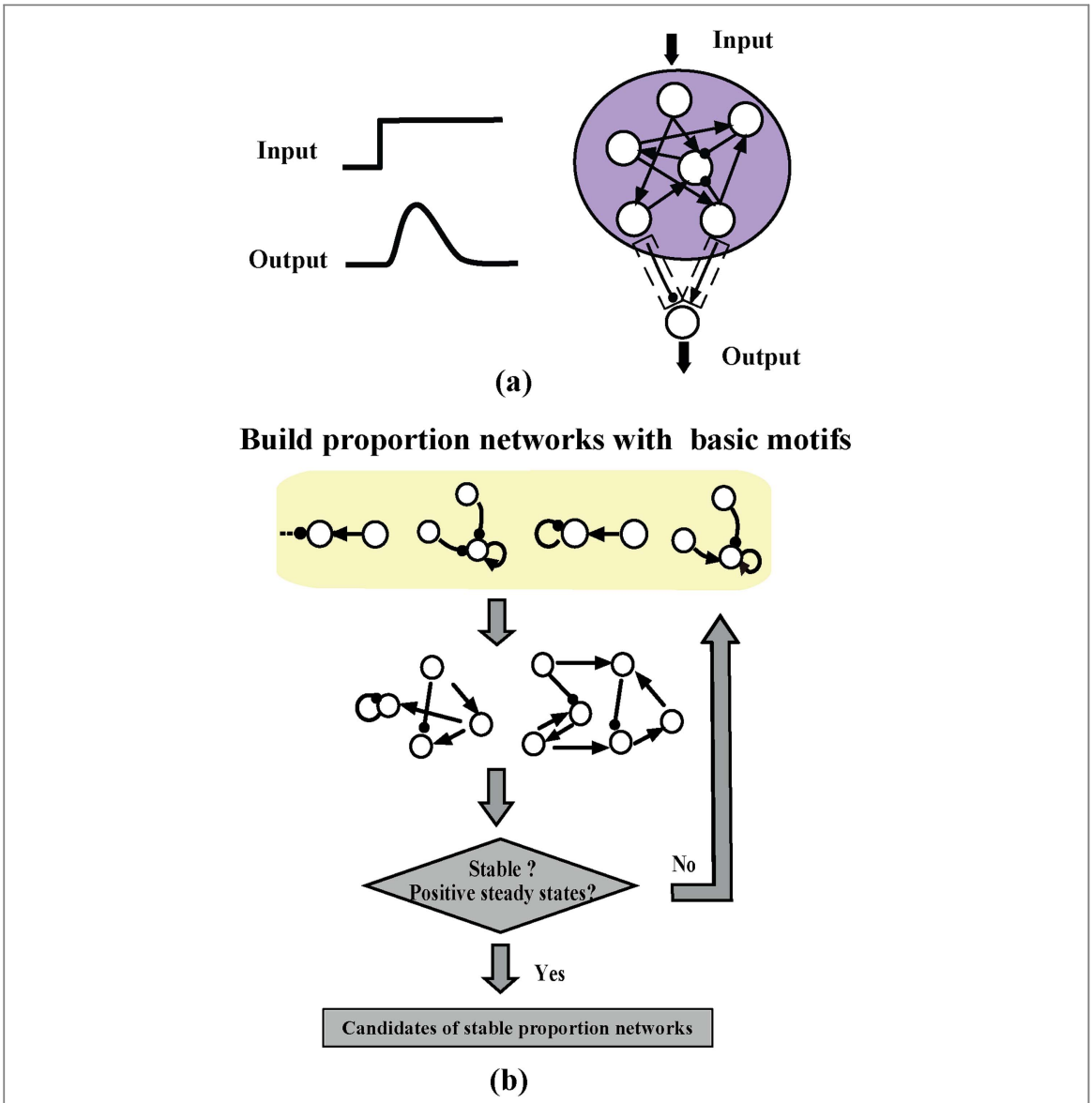

Figure 1. Schematic diagrams of adaptation and the model. (a) Dynamics of input and output for an adaptive system (left); a large network with proportional nodes controlling the output node. Nodes in the lilac circle form a proportionality sub-network and one of them receives the input. Two or more nodes from the sub-network can be used to control the output node oppositely (right). (b) The flowchart of building stable proportional networks.

networks of arbitrary size, which can be used to build adaptive networks. Here, proportional network is defined as network in which steady state concentrations of any two nodes have a proportional relationship. Analyses of these adaptive networks built from proportional networks reveal new adaptation motifs, less parameter constraints and/or more diverse dynamic features.

Methods

Specifically, we focus on enzymatic regulatory networks and model network linkages with Michaelis–Menten rate equations. In a network, each node has a fixed total concentration that can be interconverted between active and inactive forms by other active nodes or themselves. To ensure reversibility, each node has both positive (activating) and negative (inactivating) regulation. If in a network there are no positive (negative) regulations to a certain node, then a basal activating (inactivating) enzyme is assumed to act on the node. In our model, we further assume that one node (A) receives the input signal and one node (O) represents the output. If on the output node O there are two opposing regulations from node X and Y that are proportional in steady state, the output node can achieve adaptation as shown below [25]. The equation for the output node is:

$$\frac{dO}{dt} = k_{XO}X\frac{1-O}{1-O+K_{XO}} - k_{YO}Y\frac{O}{O+K_{YO}}, \quad (1)$$

where X is the activating enzyme and Y the inactivating enzyme of O. If $X^* \propto Y^*$ (* denotes steady state), then O^* depends only on the four parameters in (1). Thus, the steady state of O does not depend on the input—in

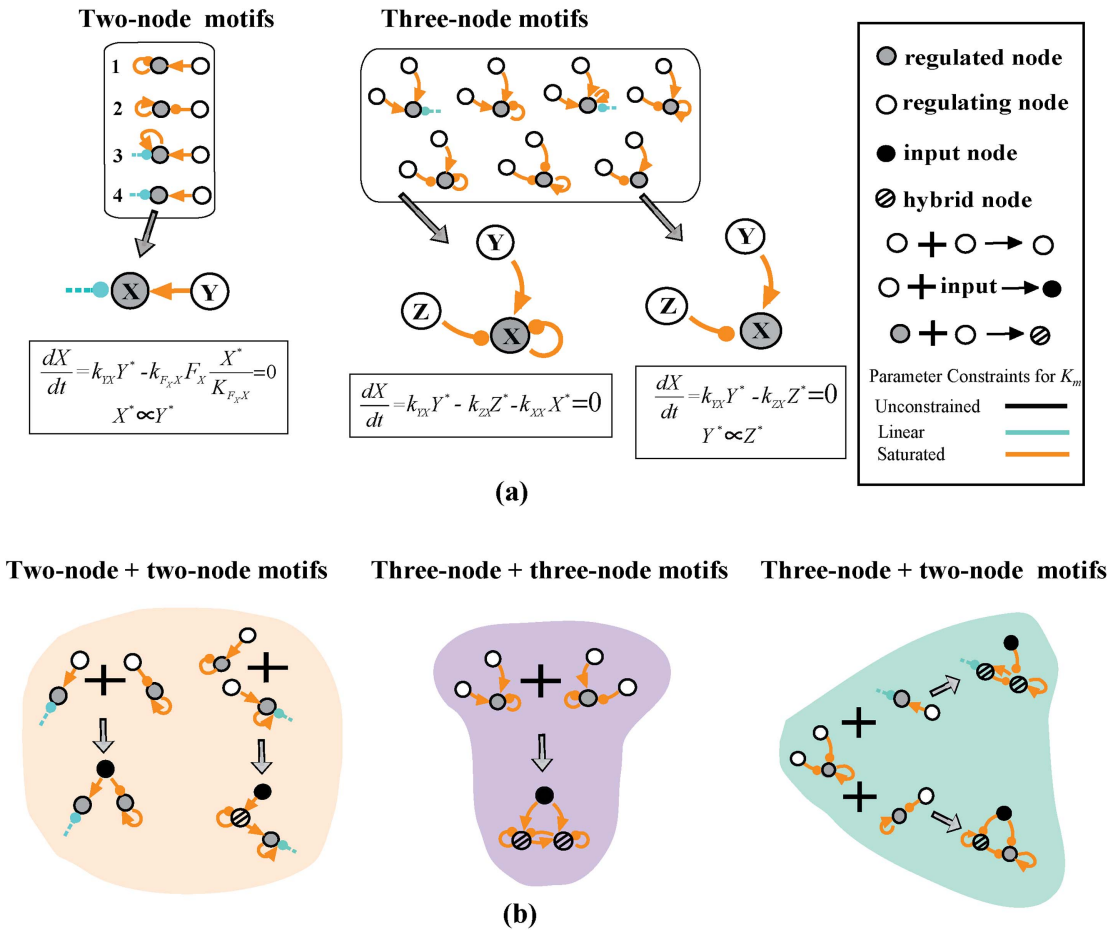

Figure 2. Basic building blocks and proportional networks built from the building blocks. (a) Basic two-node and three-node motifs with only one node is regulated. Colors of the nodes represent the categories: the regulated node (gray) and the regulating node (white). (b) Different combinations of two-node and three-node basic motifs to construct three-node proportional networks.

other words, O can adapt to input changes. Equation (1) can be easily generalized to the case in which there are multiple activating (X_i) and/or inactivating (Y_j) enzymes of O. The two terms on the right-hand side of (1) would be replaced by: $\sum_i k_{X_iO} X_i \frac{1-O}{1-O+K_{X_iO}}$ and $\sum_j k_{Y_jO} Y_j \frac{O}{O+K_{Y_jO}}$.

To construct adaptation networks of arbitrary size through the proportion mechanism, we first construct a sub-network in which all pairs of nodes have robust proportional relationships in steady state. To be robust, we mean that the relationship should not depend on details of the parameters—the enzymes should work either in the linear region or the saturated region. Adaptation on output node can be realized by assigning opposite regulations from the sub-network nodes to the output (figure 1(a)).

The construction of proportional sub-network of increasing sizes can be done hierarchically and modularly. We first identify building blocks of two and three nodes that can be used to construct small proportional networks. Larger proportional networks can then be constructed by adding additional building blocks or by combining proportional networks together. The resulting networks are checked for stability (figure 1(b)).

Results and discussion

Building blocks for proportional network

It is easy to see that if a node X is the substrate for several enzymes (which can include X itself in the case of auto-regulation), that is $\frac{dX}{dt} = F(X, Y, Z)$, then the steady state condition $F(X, Y, Z) = 0$ would establish a quantitative relationship between these enzymes and the substrate. In the case of Michaelis–Menten kinetics and if all enzymes work in the linear or saturated region, the relationship established by the steady state condition is simple and robust. In particular, with two nodes in which X is the substrate of Y, or of Y and X, the steady state condition can establish a proportional relationship between X and Y (figure 2(a) left). For three nodes in which X is the substrate, the steady state condition can establish a proportional relationship between Y and Z, or a linear relationship among X, Y and Z (figure 2(a) right). These two- and three-nodes motifs with robust proportional or linear relationships between nodes can serve as *building blocks* for the construction of proportional networks. There are four such building blocks of two-nodes and seven of three-nodes

(figure 2(a), see figures S1 and S2 for equations describing them). For convenience of later discussion, we refer the substrate node X as the regulated node and the other nodes (Y and Z) as the regulating nodes.

Constructing three-node proportional networks from building blocks

We build three-node proportional networks by combining two-node and three-node building blocks. During combination, a regulating node can combine with any other regulating node from other motifs and maintain its regulating capability; a regulating node can also combine with a regulated node from another motif and form a hybrid node. The regulated nodes cannot combine with each other among motifs. Note that for an adaptive network, there must be a node that receives the input (we refer such node as the input node). For the proportional networks combined from the building blocks, only the regulating node can serve as an input node; otherwise the input signal would enter the equation for the regulated node, disrupting the predetermined proportional or linear relationship. To simplify the stability analyses, which will be discussed later, we assume that there is no feedback to the input node from other nodes in the network.

There are three major ways of combining building blocks to construct three-node proportional networks (figure 2(b)). The first is the combination of two two-node motifs: the two motifs can share the regulating node which serves as the input node, or they can form a hybrid node. The second way is the combination of two three-node motifs. They share one regulating node which is also the input node and the other two nodes become hybrid nodes. The third way is the combination of a two-node motif and a three-node motif. In such case, one of the regulating nodes in the three-node motif is the input node. The combined network can have either one hybrid node or two hybrid nodes. After enumerating all such combinations, we are able to construct three-node proportional networks, which are then subject to stability test.

Larger proportional networks with more than three nodes can be constructed in multiple ways. Before discussing them, let us first analyze adaptation networks that are made from three-node proportional networks. Any three-node proportional network can form an adaptive four-node network by using any two or three nodes of the three-node network to oppositely regulate an output node.

Four-node adaptive networks from three-node proportional networks

When a proportional network is built with the process above, the parameters need to be tuned to guarantee that (1) the steady state of each node is positive and (2) the system is stable. If a proportional network passes the check, after assigning opposite regulations from the network nodes to an output node, the output can adapt. As an example of adaptation with the mechanism of proportion, we summarize the generation of four-node adaptive networks with three-node proportional sub-networks here.

First, we analyze the stability of the three-node proportional (node A, B and C) network. We refer node A as the node receiving input and assume that (i) there is no feedback to node A from other nodes so that the stability of the network can be determined easily, (ii) all Michaelis–Menten terms are in the linear or saturated regions such that there are no nonlinear terms in the equations. The ordinary differential equations describing such a proportional system can be written as:

$$\begin{cases} \dfrac{dA}{dt} = f_A(I, A) \\ \dfrac{dB}{dt} = f_B(A, B, C) = \beta_{AB}A + \alpha_{BB}B + \beta_{CB}C \\ \dfrac{dC}{dt} = f_C(A, B, C) = \beta_{AC}A + \beta_{BC}B + \alpha_{CC}C, \end{cases} \tag{2}$$

where we combined the parameters k_{ij} and K_{ij} into α_{ij} and β_{ij} in each term.

The Jacobian matrix of the system is

$$J = \begin{pmatrix} \dfrac{\partial f_A}{\partial A} & \dfrac{\partial f_A}{\partial B} & \dfrac{\partial f_A}{\partial C} \\ \dfrac{\partial f_B}{\partial A} & \dfrac{\partial f_B}{\partial B} & \dfrac{\partial f_B}{\partial C} \\ \dfrac{\partial f_C}{\partial A} & \dfrac{\partial f_C}{\partial B} & \dfrac{\partial f_C}{\partial C} \end{pmatrix} = \begin{pmatrix} \alpha_{AA} & 0 & 0 \\ \beta_{AB} & \alpha_{BB} & \beta_{CB} \\ \beta_{AC} & \beta_{BC} & \alpha_{CC} \end{pmatrix}. \tag{3}$$

To make the system's steady state stable, the real parts of all the eigenvalues of the Jacobian matrix should be negative, which means that $\alpha_{AA} < 0$, $\alpha_{BB} + \alpha_{CC} < 0$, $\alpha_{BB}\alpha_{CC} - \beta_{BC}\beta_{CB} > 0$. Besides, the parameters should also satisfy certain constraints to make the concentration of each node positive at steady state: $B^* = \dfrac{\beta_{CB}\beta_{AC} - \alpha_{CC}\beta_{AB}}{\alpha_{BB}\alpha_{CC} - \beta_{BC}\beta_{CB}}A^* > 0$ and $C^* = \dfrac{\beta_{BC}\beta_{AB} - \alpha_{BB}\beta_{AC}}{\alpha_{BB}\alpha_{CC} - \beta_{BC}\beta_{CB}}A^* > 0$ (see supplementary material for detailed analysis). We then choose the three-node proportional networks with such parameter constraints.

After we add an output node D to the system, four-node adaptive networks are created. In this section, we first study the adaptive networks in which input node A only regulates node B in the proportional sub-network and the output node D is only regulated by A and B. There are four classes of such topologies (figure 3): (1) incoherent feedforward loops (IFFLs), (2) the combination of an IFFL and a positive feedback loop (PFBL), (3) the combination of an IFFL and a negative feedback loop (NFBL), and (4) the combination of a coherent feedforward loop (CFFL) and a NFBL. These topologies have different dynamical characteristics. We sampled a wide range of parameters to

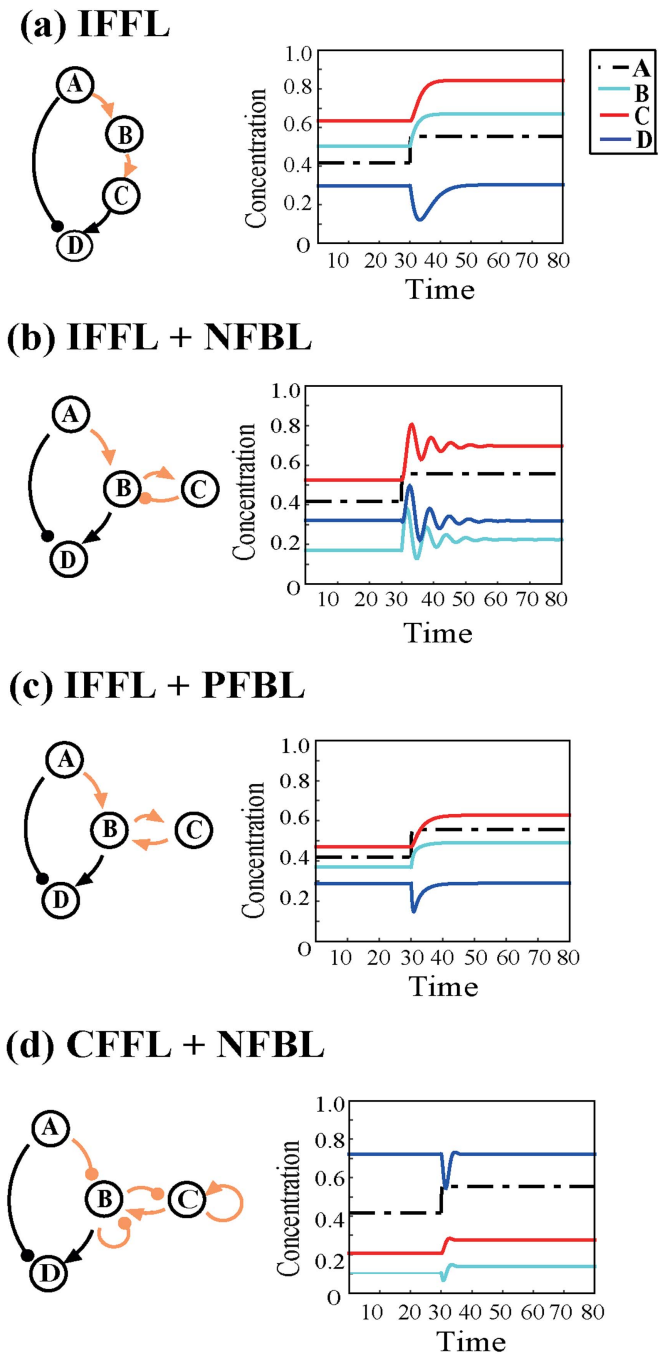

Figure 3. Four classes of four-node adaptive networks built with proportional motifs. The topologies and response dynamics of the four-node adaptive networks for (a) IFFL, (b) IFFL combined with NFBL, (c) IFFL combined with PFBL and (d) CFFL combined with NFBL. In the simulations throughout the text, input changes from 0.5 to 0.6 at time = 30. Other parameters are listed in the supplementary material.

characterize the adaptation and they behaved well under some ranges of parameter sets (figure S6). Note that for all the networks we discuss, if other nodes regulate a certain node all positively, then there is a basal enzyme inactivating this node. Such basal enzyme can be replaced by a positive self-regulation combined with an inhibitory basal enzyme (motif 3 in figure 2(a) left). Our results do not include all such replacements for simplicity. Below we analyze the networks' characteristics.

Incoherent feedforward loops

For a pure IFFL, the output node is controlled through two pathways (figure 3(a)). One is directly from the input node *A*, which has a short time scale and determines the transient response of the output when the input signal changes. The other one is a multi-step signal transduction from the input node. This pathway has a relatively longer time scale and can cancel the change of output due to the first pathway to make the network adaptive. This cascade structure contributes

to improving the sensitivity of the adaptation system by delaying the signal transmission time in the indirect pathway.

An IFFL combined with a feedback loop

An IFFL can combine a NFBL or a PFBL to yield an adaptive network (figures 3(b) and (c)). From analysis of the Jacobian matrix, the eigenvalues of the stable adaptive networks with a positive feedback are always real numbers, which means there is no damped oscillation in the behavior of such networks. However, the eigenvalues of the stable adaptive networks with a negative feedback can be complex numbers under certain parameter sets so that damped oscillations can emerge (see supplementary material). Abundant output dynamics in biological systems remain attractive puzzles, such as shift from oscillation to a sustained state or even adaptation [26–28]. The IFFL coupled NFBL may provide a flexible network to achieve multi-dynamics with corresponding parameters been tuned. Examples of simulations for each category are illustrated in figures 3(b) and (c).

A CFFL combined with a NFBL

For all the networks above, IFFLs are involved in the process of adaptation. However, we noted a special case in figure 3(d), in which a CFFL, combined with a NFBL, achieved adaptation.

In such a network, *A* inhibits *B*, so when the input changes from a low to a high value, the concentration of *A* increases and *B* decreases initially. However, when the system reaches equilibrium, the concentration of B should be proportional to that of *A* which increases with the input. This means that after a transient decrease, *B* will increase later on to a new steady state. Such a transient decrease is illustrated in figure 3(d). Because *A* inactivates *D*, and *B* activates *D*, after the change of input, the transient decrease of *B* can help *A* further inactivate *D* and thus *D* can respond to the change of input more strongly to improve the sensitivity. The CFFL topology was also found in three-node adaptive networks but with stricter parameter constraints than those of four-node ones (figure S4 and supplementary material).

Four-node adaptive networks with *A* regulating both *B* and *C*

We summarized above the features of four-node adaptive networks with only *B* regulated by *A*. We now discuss the case in which *A* regulates both *B* and *C*. Figure 4(a) lists such three-node proportional subnetworks (In the networks, if other nodes regulate a certain node all positively, and this node regulates itself negatively, then such negative self-regulation can be replaced by a basal enzyme inactivating this node or a positive self-regulation combined with an inhibitory basal enzyme; besides, for simplicity, the output node *D* is not shown) whose stability has been approved (supplementary material). Among the networks, the two pathways from *A* to *B* and from *A* to *C* can either be independent or not. When there is a negative feedback between *B* and *C*, the networks can perform a damped oscillation under certain range of parameters after the change of input. When there is no interaction between *B* and *C* or the interaction is not a negative feedback, there cannot be damped oscillations. For the networks in which *A* inactivates *B*, after the change of input, the concentration of *B* decreases transiently and then increases to reach equilibrium which is the feature of the network in figure 3(d) (see figure S5 for more architectures). Due to symmetry, the mirror images of networks in figure 4(a) are also proportional networks and are not shown here.

Another thing to be noticed is that after we construct the proportional network and adding one output node to make it achieve adaptation, such output can be regulated by any combinations of the nodes in the proportional network as long as all the regulations do not have the same signs. Examples can be seen in figure 4(b). Such characteristic can make network design more flexible with different output steady states and dynamics.

Large adaptive networks

So far we have built stable two-node and three-node proportional networks. We proceed to present two methods to construct larger proportional networks. The first is a logic extension of the two- and three-node ones. For example, if we want to build four-node proportional networks, we can identify the basic four-node motifs that can establish a linear relationship at steady state: $\kappa_X X + \kappa_Y Y + \kappa_Z Z + \kappa_W W = 0$. Then by combining one such motif with two other motifs from the motif pools of two-, three- and four-nodes, one obtains a potential four-node proportional network. Three motifs establish three relationships among the four nodes, and when solving three equations for four nodes, we could get proportionality relationship between any two of the four nodes. Such method is in principle general and can be applied to building proportional networks of arbitrary size. In practice, however, this method may not be suitable for large networks. It can be cumbersome to match motifs and it may be difficult to establish a linear relationship simultaneously involving many nodes because that would require many enzymes to regulate the same substrate.

The other method is to build large proportional networks modularly with smaller proportional networks (modules) that have already been built and shown be to stable. For example, we could design a ten-node proportional network as follows (figure 5). First, we can divide the ten nodes into different groups and each group has two or three nodes. Thus each group can form a two or three-node proportional module. Next we can link different groups to make a

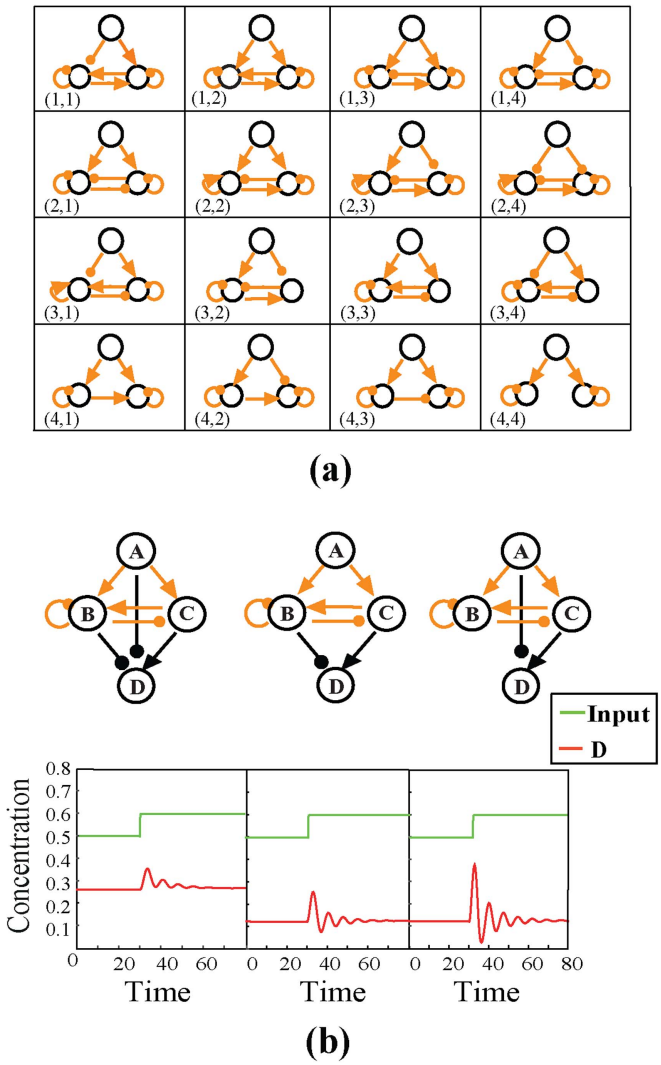

Figure 4. Networks with node *A* regulating both *B* and *C*. (a) Three-node proportional sub-networks. (b) Examples of networks in which node *D* is regulated by combinations of upstream nodes *A*, *B* and *C*. These three networks share the same proportional sub-network equations but with different output node equations. The dynamics of the three networks are shown under each network. Parameters in the simulations are listed in the supplementary material.

connected network. Because in each two-node and three-node proportional network, there is at least one node that can assume the task of receiving input, if we connect this node with any one node in another group in a way as to make these two nodes form a stable two-node motif (motif 1, 3, 4 in figure 2(a) left), then a proportional relationship can be established between these two nodes and such proportion can spread over the two connected groups. If all groups are connected this way, we would have a ten-node proportional network. Notice that there cannot be any feedback among these groups, otherwise, we have an extra proportion relationship which could contradict the proportionality that has been established. So the groups themselves can only form a directed rooted tree topology in which the input node in the root receives the external signal of the whole system. Obviously, the ten-node network can serve as a module for constructing even larger networks. Such modular design approach makes it easier to create large proportional networks from small ones that have been built. Because in the process, each group is already a stable proportional network, after we link different groups with a stable two-node motif, the stability of the whole system is guaranteed. Note also that even a system with multiple adaptive outputs with varying steady state values and dynamics can be constructed from a proportional sub-network (figure 5 bottom network). This design could help to integrate multiple nodes and/or deliver diverse outputs.

Biological examples of adaptation through proportion

There are real examples for this kind of adaptive networks. One is the adaptation of the chemotaxis signaling pathway in *Dictyostelium discoideum* (figure 6(a)). When the concentration of the chemoattractant cAMP changes, the dynamics of activated Ras, Ras-GTP shows adaptation. In the model from previous study [29–32], the cAMP signal through the

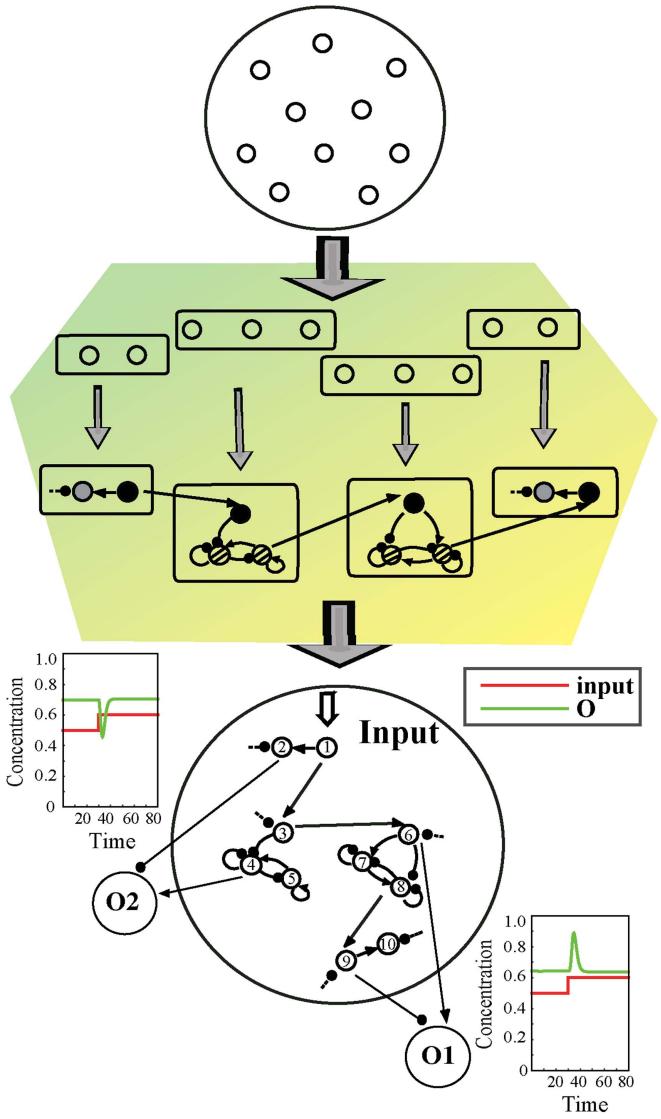

Figure 5. Larger networks built hierarchically from small proportional modules. A multiple-output adaptive network with a proportional sub-network (in the bottom circle), which is in turn built from small proportional modules. Parameters in the simulations are listed in the supplementary material.

receptor R activates both GTP-exchange factor for Ras, RasGEF and GTPase activating protein for Ras, RasGAP. While RasGEF can activate RasGTP, RasGAP can convert active RasGTP to the inactive RasGDP. Thus the system is a four-node IFFL that can achieve adaptation through the proportion mechanism among bound receptors, concentrations of RasGAP and RasGEF [33] (figure 6(a)). Such model is consistent with the local excitation, global inhibition model for gradient sensing [32] and provides experimental evidence that proportion can play a role in adaptive process.

Hill coefficient $n > 1$

So far, we have set the Hill coefficient n to be 1 to establish the proportional relationship. However, in biological world, cooperative regulations are abundant which indicates larger Hill coefficients. Previous study of three-node adaptive networks showed that Hill coefficient $n > 1$ hampers the linearity required to establish the proportional relationship necessary in the IFFLP class [25]. We note that this restriction on Hill coefficient ($n = 1$) can be relaxed in larger adaptive networks, as with more nodes proportional relationships could be established between powers of concentrations. For example, in the biological example above (figure 6(a)), as long as the two intermediate nodes are regulated with the same Hill coefficient, they can still form a proportional relationship and make the output adapt.

To further illustrate how Hill coefficients $n > 1$ can exist in proportional adaptive networks, we analyze another example shown in figure 6(b) (left). Let us assume the equations for nodes B and C are:

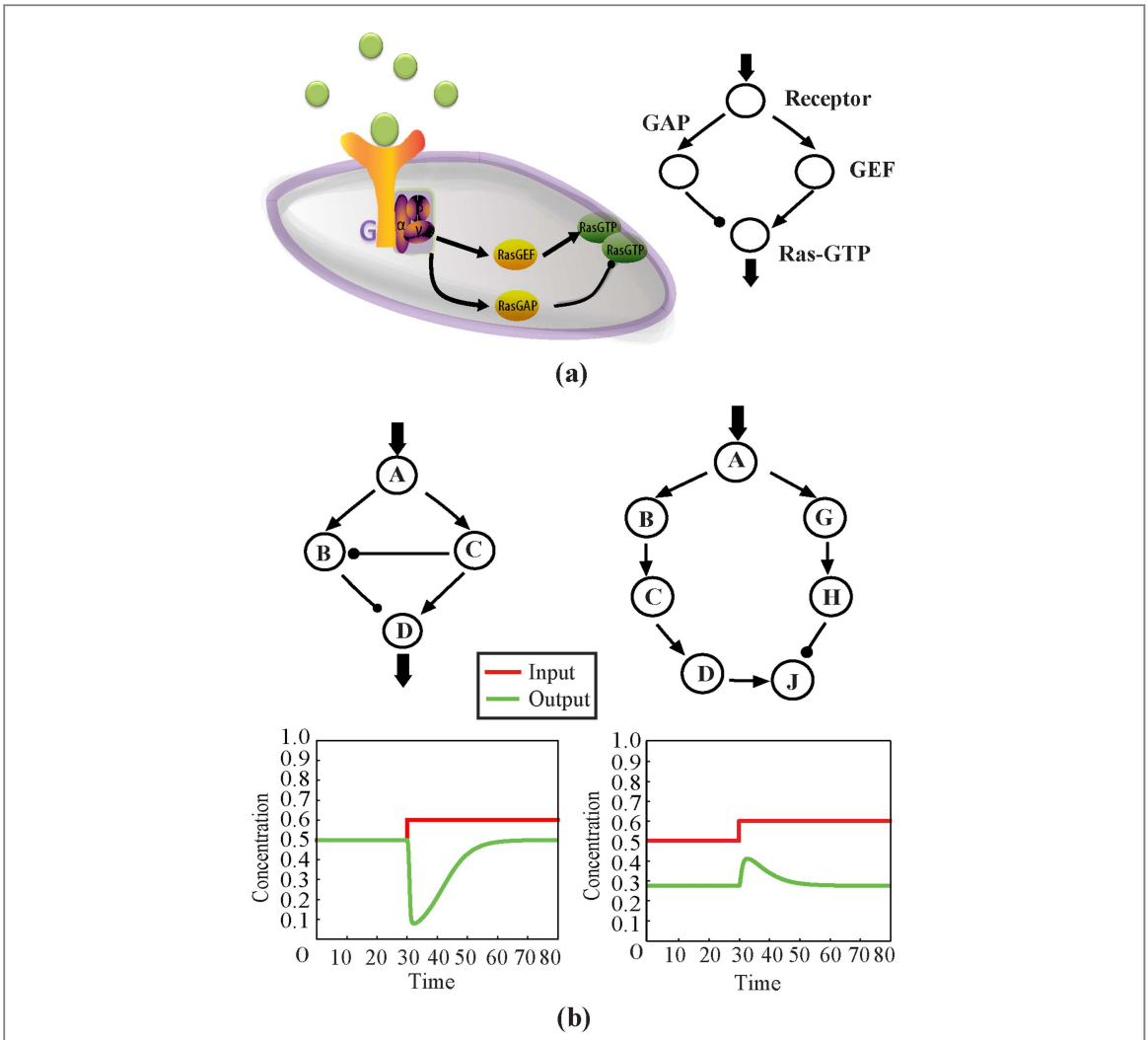

Figure 6. A biological example of a proportional adaptive network and adaptive networks with different Hill coefficients. (a) Chemotaxis signaling pathway in *Dictyostelium discoideum* and the simplified network. (b) A four-node and a seven-node adaptive network with Hill coefficient larger than 1. Parameters in the simulations are listed in the supplementary material.

$$\begin{aligned}\frac{\mathrm{d}B}{\mathrm{d}t} &= k_{AB}A\frac{1-B}{1-B+K_{AB}} - k_{CB}C\frac{B^{n_B}}{B^{n_B}+K_{CB}^{n_B}}\\ \frac{\mathrm{d}C}{\mathrm{d}t} &= k_{AC}A\frac{1-C}{1-C+K_{AC}} - k_{F_CC}F_C\frac{C^{n_C}}{C^{n_C}+K_{F_CC}^{n_C}}.\end{aligned} \tag{4}$$

If the first terms on the right-hand sides in both equations are in the saturated region and the second terms are in the linear region, then $A^* \propto C^* B^{*n_B}$ and $A^* \propto C^{*n_C}$, leading to $B^{*n_B} \propto C^{*n_C-1}$. When $n_B = n_C - 1$, $B^* \propto C^*$ makes the output node adapt. When the condition $n_B = n_C - 1$ is not strictly satisfied, the system could not achieve perfect adaptation (figure S7).

With more nodes, one could have more choices and combinations of Hill coefficients. Consider a seven-node network shown in figure 6(b) (right):

$$\begin{aligned}\frac{\mathrm{d}B}{\mathrm{d}t} &= k_{AB}A\frac{1-B}{1-B+K_{AB}} - k_{F_BB}F_B\frac{B^{n_B}}{B^{n_B}+K_{F_BB}^{n_B}}\\ \frac{\mathrm{d}C}{\mathrm{d}t} &= k_{BC}B\frac{1-C}{1-C+K_{BC}} - k_{F_CC}F_C\frac{C^{n_C}}{C^{n_C}+K_{F_CC}^{n_C}}\\ \frac{\mathrm{d}D}{\mathrm{d}t} &= k_{CD}C\frac{1-D}{1-D+K_{CD}} - k_{F_DD}F_D\frac{D^{n_D}}{D^{n_D}+K_{F_DD}^{n_D}}\\ \frac{\mathrm{d}G}{\mathrm{d}t} &= k_{AG}A\frac{1-G}{1-G+K_{AG}} - k_{F_GG}F_G\frac{G^{n_G}}{G^{n_G}+K_{F_GG}^{n_G}}\end{aligned}$$

$$\begin{aligned}\frac{dH}{dt} &= k_{GH}G\frac{1-H}{1-H+K_{GH}} \\ &\quad - k_{F_HH}F_H\frac{H^{n_H}}{H^{n_H}+K_{F_HH}^{n_H}} \\ \frac{dJ}{dt} &= k_{DJ}D\frac{1-J}{1-J+K_{DJ}} \\ &\quad - k_{HJ}H\frac{J}{J+K_{HJ}},\end{aligned} \tag{5}$$

where F_i is basal inactivating enzyme for node i. If the first terms on the right-hand sides in equations describing nodes B to H are in the saturated region and the second terms are in the linear region, then $A^* \propto B^{*n_B}$, $B^* \propto C^{*n_C}$, $C^* \propto D^{*n_D}$, $A^* \propto G^{*n_G}$ and $G^* \propto H^{*n_H}$, lead to $A^* \propto D^{*n_Bn_Cn_D}$, $A^* \propto H^{*n_Gn_H}$. When $n_Bn_Cn_D = n_Gn_H$, $D \propto H$ leads to the adaptation of the output node J. Similarly, when the Hill coefficients deviate from the strict condition for perfect adaptation, the system's ability to adapt decreases (figure S8).

Conclusion

Understanding how complex biological networks carry out sophisticated regulatory functions is a major goal in systems biology, in which computational approaches have been playing a unique, indispensable and increasingly critical role. A deeper quantitative understanding towards this end can also provide useful tools for synthetic biologists. Previous study on three-node enzymatic networks revealed two robust solutions that can achieve perfect adaptation: NFFLB and IFFLP [25]. In an extensive search for four-node adaptive networks using an evolutionary algorithm (data not shown), we found repeatedly adaptive networks with two or more nodes forming a proportionality sub-network, which can be viewed as a generalization of the IFFLP mechanism. These results inspired us to perform the current systematic study on constructing adaptive networks from proportionality sub-networks. There are many ways to form proportionality networks of different sizes. Instead of enumerating them, we focused on the methodology of building them up using basic motifs and modules. Self-consistent combinations of motifs and modules can generate larger and larger proportional and adaptive networks. Our results significantly enriched the repertoire of adaptive networks of larger sizes. We analyzed some example networks and found that they display a variety of rich dynamic features as well as more relaxed parameter constraints.

Proportional relationship can play important roles in adaptive networks with other regulatory forms, e.g. transcriptional regulation (supplementary material), or in functions other than adaptation, such as circadian clocks [34] and stress-responsive pathways [35]. How cells generate and regulate the proportional relationship in various settings are of general interest. Investigators have used the approach of synthetic biology to synthesize adaptive networks based on the IFFLP motif [36]. The networks studied in this paper provide a rich toolbox for constructing proportional and adaptive networks. Besides, when synthetic biology is aiming at constructing larger and more complicated functional networks, how to coordinate different modules and components becomes one of the key points. In the bottom-up module-design approach we provide here, different components are coordinated to create large-scale networks performing adaptation robustly without disrupting each module whose proportionality is still remained. These results not only shed light in understanding natural adaptive networks, but also provide a systematic tool for designing synthetic networks of versatile functional features.

Author contributions

Conceived and designed the projects: CT. Performed analytic analysis: LX WS. Developed the computational models: LX WS. Conducted the simulation: WS LX. Wrote the manuscript: LX WS CT.

Acknowledgments

We thank Shouwen Wang and Wenzhe Ma for helpful discussions, Iain Bruce for detailed proofreading of the manuscript. The work was supported by Chinese Ministry of Science and Technology (2015CB910300) and National Natural Science Foundation of China (91430217). LX acknowledges the support from the National Undergraduate Training Program for Innovation and Entrepreneurship of China.

References

[1] Gardner T S, Cantor C R and Collins J J 2000 Construction of a genetic toggle switch in *Escherichia coli Nature* **403** 339–42
[2] Yao G, Lee T J, Mori S, Nevins J R and You L C 2008 A bistable Rb-E2F switch underlies the restriction point *Nat. Cell Biol.* **10** 476–82
[3] Elowitz M B and Leibler S 2000 A synthetic oscillatory network of transcriptional regulators *Nature* **403** 335–8
[4] Tsai T Y C, Choi Y S, Ma W Z, Pomerening J R, Tang C and Ferrell J E 2008 Robust, tunable biological oscillations from interlinked positive and negative feedback loops *Science* **321** 126–9
[5] Ma W Z, Lai L H, Qi O Y and Tang C 2006 Robustness and modular design of the Drosophila segment polarity network *Mol. Syst. Biol.* **2** 70
[6] Chau A H, Walter J M, Gerardin J, Tang C and Lim W A 2012 Designing synthetic regulatory networks capable of self-organizing cell polarization *Cell* **151** 320–32
[7] Hornung G and Barkai N 2008 Noise propagation and signaling sensitivity in biological networks: a role for positive feedback *PloS Comput. Biol.* **4** e8
[8] Yang X J, Lau K Y, Sevim V and Tang C 2013 Design principles of the yeast G1/S switch *PloS Biol.* **11** e1001673
[9] Ping X F and Tang C 2015 An atlas of network topologies reveals design principles for caenorhabditis elegans vulval precursor cell fate patterning *PloS One* **10** e0131397
[10] Brandman O, Ferrett J E, Li R and Meyer T 2005 Interlinked fast and slow positive feedback loops drive reliable cell decisions *Science* **310** 496–8

[11] Wagner A 2005 Circuit topology and the evolution of robustness in two-gene circadian oscillators *Proc. Natl Acad. Sci. USA* **102** 11775–80
[12] Yao G, Tan C, West M, Nevins J R and You L 2011 Origin of bistability underlying mammalian cell cycle entry *Mol. Syst. Biol.* **7** 485
[13] Kirsch M L, Peters P D, Hanlon D W, Kirby J R and Ordal G W 1993 Chemotactic methylesterase promotes adaptation to high concentrations of attractant in Bacillus subtilis *J. Biol. Chem.* **268** 18610–6
[14] Marshall C 1995 Specificity of receptor tyrosine kinase signaling: transient versus sustained extracellular signal-regulated kinase activation *Cell* **80** 179–85
[15] Barkal N and Leibler S 1997 Robustness in simple biochemical networks *Nature* **387** 913–7
[16] Matthews H R and Reisert J 2003 Calcium, the two-faced messenger of olfactory transduction and adaptation *Curr. Opin. Neurobiol.* **13** 469–75
[17] Mello B A and Tu Y 2003 Quantitative modeling of sensitivity in bacterial chemotaxis: the role of coupling among different chemoreceptor species *Proc. Natl Acad. Sci.* **100** 8223–8
[18] Rao C V, Kirby J R and Arkin A P 2004 Design and diversity in bacterial chemotaxis: a comparative study in *Escherichia coli* and Bacillus subtilis *PLoS Biol.* **2** E49–49
[19] Kollmann M, Løvdok L, Bartholomé K, Timmer J and Sourjik V 2005 Design principles of a bacterial signalling network *Nature* **438** 504–7
[20] Endres R G and Wingreen N S 2006 Precise adaptation in bacterial chemotaxis through 'assistance neighborhoods *Proc. Natl Acad. Sci.* **103** 13040–4
[21] Yang L and Iglesias P A 2006 Positive feedback may cause the biphasic response observed in the chemoattractant-induced response of Dictyostelium cells *Syst. Control Lett.* **55** 329–37
[22] Mettetal J T, Muzzey D, Gómez-Uribe C and van Oudenaarden A 2008 The frequency dependence of osmo-adaptation in Saccharomyces cerevisiae *Science* **319** 482–4
[23] Behar M, Hao N, Dohlman H G and Elston T C 2007 Mathematical and computational analysis of adaptation via feedback inhibition in signal transduction pathways *Biophys. J.* **93** 806–21
[24] François P and Siggia E D 2008 A case study of evolutionary computation of biochemical adaptation *Phys. Biol.* **5** 026009
[25] Ma W, Trusina A, El-Samad H, Lim W A and Tang C 2009 Defining network topologies that can achieve biochemical adaptation *Cell* **138** 760–73
[26] Suel G M, Kulkarni R P, Dworkin J, Garcia-Ojalvo J and Elowitz M B 2007 Tunability and noise dependence in differentiation dynamics *Science* **315** 1716–9
[27] Geva-Zatorsky N *et al* 2006 Oscillations and variability in the p53 system *Mol. Syst. Biol.* **2** 006.0033
[28] Hao N, Budnik B A, Gunawardena J and O'Shea E K 2013 Tunable signal processing through modular control of transcription factor translocation *Science* **339** 460–4
[29] Jin T 2013 Gradient sensing during chemotaxis *Curr. Opin. Cell Biol.* **25** 532–7
[30] Skoge M, Yue H C, Erickstad M, Bae A, Levine H, Groisman A, Loomis W F and Rappel W J 2014 Cellular memory in eukaryotic chemotaxis *Proc. Natl Acad. Sci. USA* **111** 14448–53
[31] Levine H and Rappel W J 2013 The physics of eukaryotic chemotaxis *Phys. Today* **66** 24–30
[32] Chang H and Levchenko A 2013 Adaptive molecular networks controlling chemotactic migration: dynamic inputs and selection of the network architecture *Phil. Trans. R. Soc.* B **368** 20130117
[33] Takeda K, Shao D Y, Adler M, Charest P G, Loomis W F, Levine H, Groisman A, Rappel W J and Firtel R A 2012 Incoherent feedforward control governs adaptation of activated ras in a eukaryotic chemotaxis pathway *Sci. Signal.* **5** ra2
[34] Kim J K and Forger D B 2012 A mechanism for robust circadian timekeeping via stoichiometric balance *Mol. Syst. Biol.* **8** 630
[35] Stewart-Ornstein J, Nelson C, DeRisi J, Weissman J S and El-Samad H 2013 Msn2 coordinates a stoichiometric gene expression program *Curr. Biol.* **23** 2336–45
[36] Bleris L, Xie Z, Glass D, Adadey A, Sontag E and Benenson Y 2011 Synthetic incoherent feedforward circuits show adaptation to the amount of their genetic template *Mol. Syst. Biol.* **7** 519